Proceedings Paper:
Tsang, C., Bingham, C., Foster, M.P. et al. (2016) Minimum charge-recovery time control with parallel connected buck converters. In: The 8th IET International Conference on Power Electronics, Machines and Drives (PEMD) 2016. IET Power Electronics, Machines and Drives Conference 2016, 19 – 21 April 2016 , Glasgow, UK. Institution of Engineering and Technology. ISBN: 978-1-78561-188-9.

https://doi.org/10.1049/cp.2016.0155

Minimum charge-recovery time control with parallel connected buck converters

[†]C. –W. Tsang, [†]C. Bingham, [††]M.P. Foster, [††]D.A. Stone, [††]J.N. Davidson [†††]J.M.Leach*

[†]*University of Lincoln, Lincoln School of Engineering, Brayford Pool, Lincoln, UK*
[††]Electronic and Electrical Engineering, The University of Sheffield, Sheffield, UK
[†††]*Castlet Ltd, 14 Crofton Drive,Allenby Road Inductrial Estate, Lincoln, UK*
**Email: ctsang@lincoln.ac.uk*

Keywords: Minimum charge recovery time control, parallel converter, buck converter, coupled inductor.

Abstract

Optimal-time control to minimise a converter's recovery time has thus far been reported only for single power module converters. This paper adapts the optimal-time control problem and applies it to converters based on multiple power modules. Additionally, a novel minimum charge-recovery time control is also proposed for the multiple power module converter which produces a recovery time shorter than that in the optimal-time control. A 20 W converter is used to demonstrate the improved characteristics under primary regions of operation. Results show that the transient recovery time during a load step change is improved by 75% compared to traditional optimal time control.

1 Introduction

With the broadening scope of application for DC-DC converters, research to develop topologies with high-bandwidth transient responses and high-efficiency operation, is intensifying. The slew-rate of buck converters is primarily limited by their inductors, and methods based on increasing the voltage across the inductor or changing the inductance value during transient conditions, have been reported [1,2] to improve the transient response. One example is the augmented converter [3], where a resistive path is enabled during the transient condition to allow extra charge to be provided to the load or absorbed by a dummy burden resistor. Although this modification improves the response time, it is at the expense of efficiency. A more effective method of increasing the slew rate is to connect an additional converter in parallel and use a one-cycle optimal-time control scheme [4]. In the case of a load step-up condition being detected, Fig. 1 shows that both the main and auxiliary power modules duty cycles are set to maximum. While the main power module (PM) duty cycle remains at the maximum until its current, $I_{\mathrm{L(m)}}$, has reached the new required level, the auxiliary PM duty cycle is reduced to zero at some desired instant (t_2 as shown in the example) such that the charge lost due to the limited slew rate is replenish at the end of the main PM current recovery. Of particular note is that the auxiliary PM current $I_{\mathrm{L(x)}}$ falls to zero as $I_{\mathrm{L(m)}}$ reaches the steady state level.

The current slew rates under the maximum and minimum duty cycles are fixed by the inductor value and therefore the voltage across the inductor, the one-cycle optimal-time control is achieved only when $L_r = V_r$ is satisfied (i.e. $L_r = L_x/L_m$ and $V_r = V_o/V_i$).

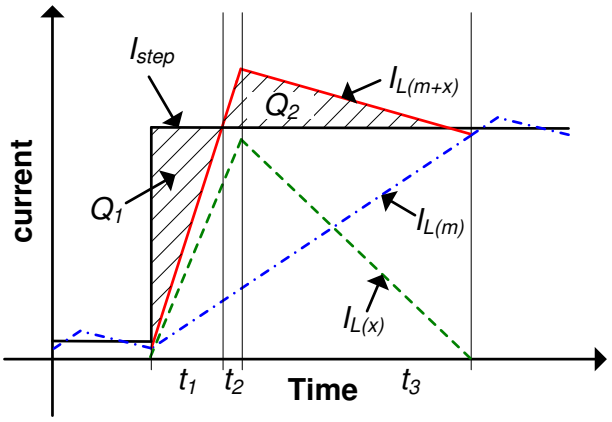

Fig. 1: Current waveforms of one-cycle optimal-time control.

In the case where $L_r < V_r$, one cycle optimal-time control cannot be achieved because the auxiliary PM current falls to zero more rapidly than that of the main PM current settling to the new desired level. Through careful selection of the auxiliary PM duty cycle, it is shown in this paper that the optimal-time control can be achieved for $L_r < V_r$.

To further improve the transient response, the paper also proposes the use of a variable inductor to reduce the charge-recovery period—termed minimum charge-recovery time control. Two methods of changing the inductance electrically have been reported in literature. Using the step-inductance technique [5], the inductance is effectively removed by short-circuiting the secondary winding of a coupled inductor. Whilst when employing the variable inductance method, the inductance is reduced by adjusting a biasing current in an additional winding on the inductor. Due to the transient nature of the proposed converter, the coupled inductor used in the stepping inductor method is proposed here to achieve the minimum charger-recovery time control.

2 Parallel connect buck converter

The proposed parallel-connected synchronous buck converter (SBC) with a coupled inductor, is shown in Fig. 2. The design of the converter involves the selection of the switching frequencies os switches S_1, S_2, S_3 and S_4 (i.e. S_1, is switched complementarily to S_2, similarly S_3 is switched complementarily to S_4), the LC low-pass filters L_m, L_x and C, and the coupled inductor L_{co} that satisfy both the steady-state ripple and transient response requirements.

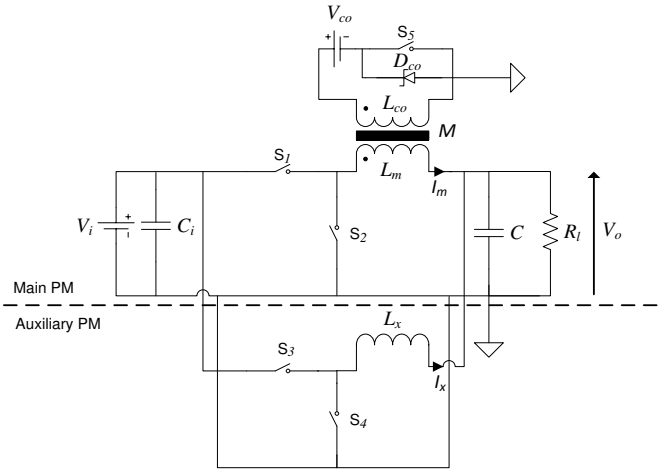

Fig. 2: Parallel connected SBC with coupled inductor.

With the coupled inductor inactive, the main PM operates as a classical SBC, and consequently has two states of continuous conduction mode (CCM) operation. During the on-state, with S_1 switched on, the inductor currents rise at the rate given in (1), whereas in the off-state, with S_2 switched off, the inductor currents fall at a rate given in (2):

$$\frac{d}{dt}I_{(+)} = \frac{V_i - V_o}{L_m} \tag{1}$$

$$\frac{d}{dt}I_{(-)} = \frac{-V_o}{L_m} \tag{2}$$

During steady-state, only the main PM is utilised, and the current rise in (1) during the on-period is identical to current fall in (2) during the off-period. Equating the two periods provides the output voltage relationship in (3), which shows that the specific duty cycle, δ_m, must be selected for the desired output voltage.

$$\delta_m = V_o/V_i \tag{3}$$

By multiplying the current rise in (1) by the on-period, the main PM current ripple, ΔI_m, can be found (4):

$$\Delta I_m = \frac{V_i(1-\delta_m)}{L_m}\delta_m t_{sm} \tag{4}$$

During transient condition, the auxiliary PM is also utilised to provide the extra charge necessary to improve the recovery time. With the output voltage maintained by the main PM, the auxiliary PM duty cycle, δ_x, is not restricted. Subtracting the current rise during the on-period from the fall during the off-period, the net current rise or fall over a switching period can be found as in (5). The auxiliary PM net current rate is positive for $\delta_x > \delta_m$ and is negative for $\delta_x < \delta_m$.

$$\frac{d}{dt}I_{x(net)} = \frac{V_i\delta_x - V_o}{L_x} \tag{5}$$

The auxiliary PM current ripple is shown in [25] to be:

$$\Delta I_x = \frac{V_i(1-\delta_x)}{L_x}\delta_x t_{sx} \tag{6}$$

To improve the charge recovery time, an inductor L_{co} is coupled to the main PM (or the auxiliary PM) inductor. When S_{co} is switched on, the current in L_{co} increases due to V_{co}. Due to the coupling between the two inductors, the change in current in one inductor affects the other according to:

$$\begin{bmatrix} V_{Lm} \\ V_{Lco} \end{bmatrix} = \begin{bmatrix} L_m & M \\ M & L_{co} \end{bmatrix} \begin{bmatrix} \frac{dI_m}{dt} \\ \frac{dI_{co}}{dt} \end{bmatrix} \tag{7}$$

where M is the mutual inductor of the coupled inductor, which can be found by (8) given the coupling coefficient k:

$$M = k\sqrt{L_m L_{co}} \tag{8}$$

Rearranging and substituting the two state equations in terms of dI_m/dt, the current rate of the main PM with coupled inductor can be calculated:

$$\frac{d}{dt}I_{m(co)} = \frac{M^2 V_c - L_m V_m}{M^2 - L_m L_{co}} \tag{9}$$

2.1 Mode of operation

In response to a step load transient, the switches are controlled to produce the following three operating modes for the different control schemes proposed in this paper. In mode 1, Fig. 3 (a), both the main and auxiliary PMs are active with the duty cycles set at the maximum, while the coupled inductor is disabled. The combined current slew rate is described by:

$$\frac{d}{dt}I_{mx(+)} = \frac{d}{dt}I_{m(+)} + \frac{d}{dt}I_{x(+)} \tag{10}$$

In mode 2, Fig. 3 (b), the main PM duty cycle is at the maximum while the auxiliary PM is set to the minimum, the current slew rate can be found by:

$$\frac{d}{dt}I_{mx(-)} = \frac{d}{dt}I_{x(net-)} - \frac{d}{dt}I_{m(+)} \tag{11}$$

In modes 3 and mode 4, both the main and auxiliary PM duty cycles are set to maximum and S_5 is switched on in mode 3, Fig. 3 (c) and is off in mode 4, the current slew rate for both operating mode are determined by:

$$\frac{d}{dt}I_{mx(co+)} = \frac{d}{dt}I_{m(co+)} + \frac{d}{dt}I_{x(+)} \tag{12}$$

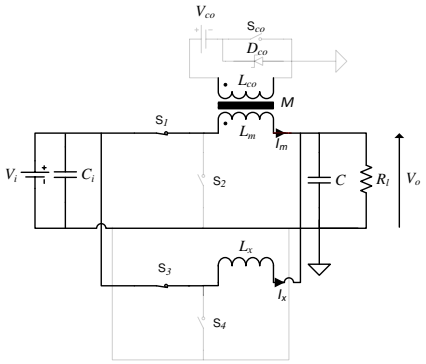

(a) – Mode 1

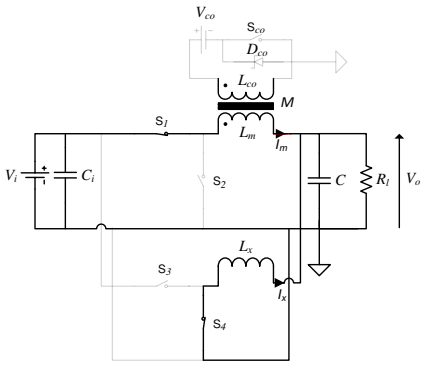

(b) – Mode 2

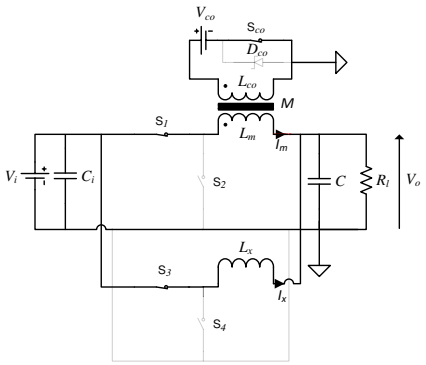

(c) – Mode 3

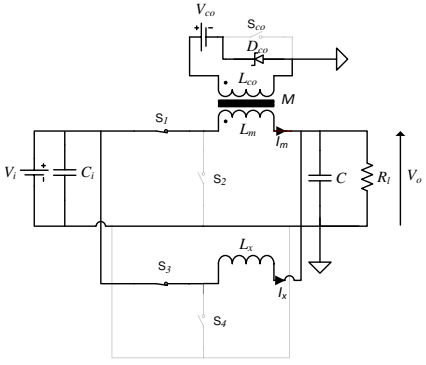

(d) – Mode 4

Fig. 3: Circuit modes of operation under load step up.

2.2 Component selection

The main PM inductor is selected to satisfy the steady-state current ripple requirement which can be calculated using (4) and the auxiliary PM is selected to achieve the desired recovery time. The inductor L_{co} is chosen to minimise winding loss, leading to the requirement for selecting the mutual inductor by solving the quadratic equation in (13), obtained by rearranging (7):

$$M^2 \frac{di_m}{dt} - V_{Lco} M + L_2 \left(V_1 - L_1 \frac{di_1}{dt} \right) = 0 \qquad (13)$$

The capacitance is selected to satisfy both the steady-state voltage ripple and transient overshoot. The latter usually resulting a higher capacitance, is given by:

$$C \geq \frac{LI_{step}{}^2}{2V_o V_{over}} \qquad (14)$$

Having selected suitable components, a control scheme is required to achieve optimal time and charge balance.

3 Optimal-time and charge balance control

To achieve charge balance control in a multi-module converter with $L_r < V_r$, as in Fig. 4, the auxiliary PM inductor current reduction rate must be selected through the choice of duty cycle range. For brevity, only a load step-up condition is considered in the following discussion, but can be readily extended to accommodate load step-down as necessary.

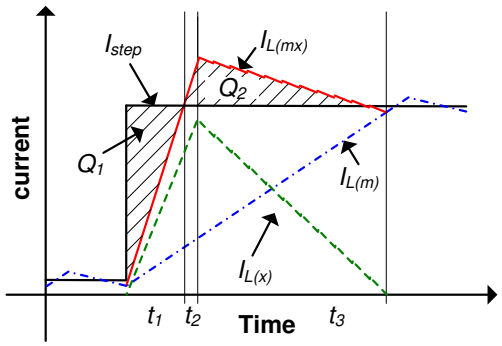

Fig. 4: Current waveforms of charge-balance control.

During t_1, the duty cycle of the two PMs are set to the maximum to: 1) bring the resulting current (solid line) to the new level as soon as possible, and 2) minimise the charge lost Q_1 to the load. The primary PM duty cycle remains at the maximum until the end of t_3, to bring the PM current (dash-dot line) to the new steady-state level in the minimum time. In order to return the auxiliary PM current (dashed line) to zero and recover the lost charge at the end of t_3, the auxiliary PM duty cycle is reduced at the end of t_2. The converter is operating in mode 1 during t_1 and t_2 and is in mode 2 during t_3.

From the geometry, and using (10) and (11), charge balance is achieved when the auxiliary PM inductor current fall rate is:

$$\frac{d}{dt} I_{x(net-)} = \frac{V_i - V_o}{L_m - L_x} \qquad (15)$$

After substituting (5) into (15), the duty cycle which produces the desired rate is found from:

$$\delta_x = \frac{L_r + V_r(1-2L_r)}{1-L_r} \tag{16}$$

From Fig. 4, the transient recovery time is determined by the main PM only, which can be found by:

$$t_{re} = \frac{L_m I_{step}}{V_i - V_o} \tag{17}$$

With the output voltage returning to its steady-state value as soon as all the charge is recovered, a faster transient recovery time is achieved by allowing the charge to be replenished at the maximum rate, as shown in Fig. 5.

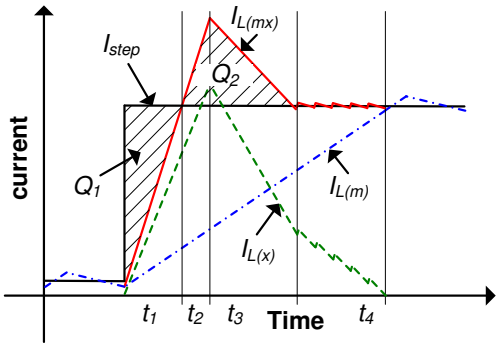

Fig. 5: Current waveforms of optimal-time control.

To achieve optimal-time control, the main and auxiliary PM duty cycles are set to maximum during t_1 and t_2. The main PM duty cycle remains unchanged while the auxiliary PM duty cycle is reduced to the minimum at the end of t_2, to allow charge-balance to be achieved at the end of t_3. The converter is operating in mode 1 in t_1 and t_2 and is in mode 2 during t_3 and t_4. By balancing the two charges $(Q_1 = Q_2)$, the recovery time seen by the load can be calculated as followed:

$$t_{re} = \frac{L_m I_{step}}{V_i - V_o}\left(\frac{L_r}{L_r+1} + \frac{1}{\sqrt{1+\frac{(V_r+1)(1-L_r)}{V_r+L_r(V_r-1)}}}\left(\frac{L_r}{L_r+1} + \frac{L_r(1-V_r)}{V_r L_r + V_r - L_r}\right)\right) \tag{18}$$

Beyond t_3 all the charge is recovered. To keep the output voltage at the steady-state value, the auxiliary PM duty cycle must be increased to match the rate of main PM:

$$\frac{d}{dt} I_{x(net-)} = \frac{V_i - V_o}{L_m} \tag{19}$$

After substituting (5) into (19), the auxiliary PM duty cycle in this period is given by:

$$\delta_x = V_r + L_r(1 - V_r) \tag{20}$$

Transient recovery is achieved at the end of t_4 which is given by (17). The recovery time of the converter with the optimal-time control (6), normalised with respect to the recovery time under the charge-balance control (5), is plotted in Fig. 5. Whilst the voltage ratio determines the minimum inductor ratio (i.e. $L_r < V_r$), the inductor ratio determines the recovery time reduction. The smaller the inductor ratio, the greater the reduction, and the higher the inductor ratio the better the resulting improvement in the transient response.

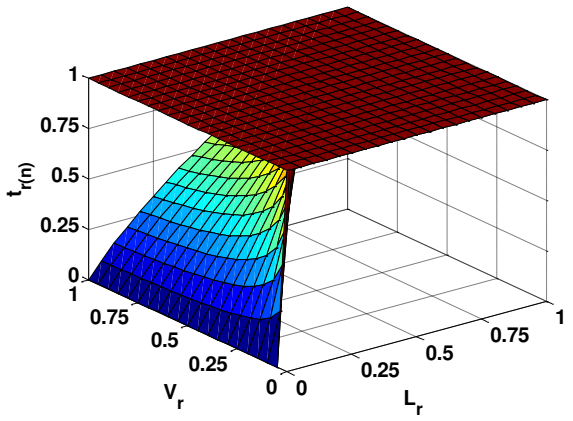

Fig. 6: Recovery time of charge-balance control and optimal time control.

3.1 Minimum charge-recovery time control

In optimal-time control, the charge Q_2 is accumulated over two periods at an increasing rate during t_2 (as described by (15)) and a reducing rate during t_3 (as described by (16)). In a converter with high voltage conversion ratio, the low current rate of reduction lengthens the period t_3, leading to a longer charge recovery period. This limitation can be overcome by replacing one of the PM inductors with a coupled inductor (more detail to be follow) which allows a higher bandwidth current rate of fall through switching off the coupled winding, and reducing t_3, as shown in Fig. 7.

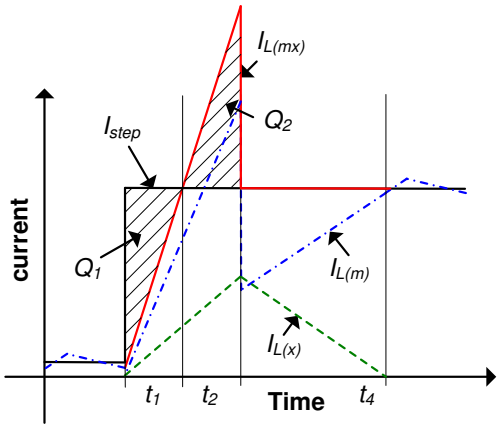

(a)

Fig. 7: Current waveforms of minimum charge-recovery time control.

With the duty cycle of both PMs set to maximum, the charge Q_2 accumulated during t_2 at the maximum rate achievable by the two inductors, the charge recovery time is reduced to the theoretical minimum; hence is termed the minimum charge-recovery time control. The auxiliary PM duty cycle in t_4 is set to match the main PM current rate as in the optimal-time control by (5).

Through symmetry, the charge recovery time is twice the time the converter takes to reach the new current level, and is given by (28).

$$t_{re(mcr)} = \frac{L_m I_{step}}{V_i - V_o}\left(\frac{2L_r}{L_r+1}\right) \quad (21)$$

The normalised charge recovery time with the minimum charge-recovery time control is shown in Fig. 8. Result shows that the recovery time is independent to the inductor ratio, being shorter with a lower inductor ratio. Under high inductor and voltage ratios, the recovery time approaches that in the optimal-time control.

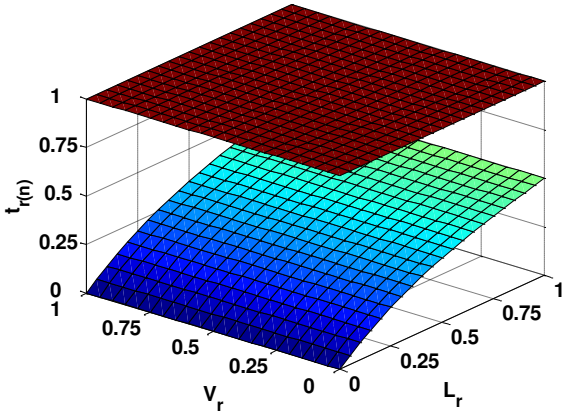

Fig. 8: Recovery time of charge-balance control and minimum recovery time control.

4 Design examples

To show the improvement in recovery time with the proposed converter scheme, a prototype with a power rating of 20 W is designed. The input and output voltages are 12 V and 3.3 V, respectively; the current ripple is selected to be 0.5 A and the voltage under- and over-shoot are to be 5% of the steady-state voltage in the worst operating condition. The minimum load current is 0.5 A and the maximum current step is 5.5 A. With the primary PM switching frequency selected to be 50 kHz, the main PM inductance is calculated from (1), to be 96 µH, and the capacitance to be 200 µF.

4.1 Simulation in Simulation

The transient responses of the converter subjected to load step-up and down are shown, respectively, in Fig. 9 (a) and (b). The results show that whilst the transient recovery under the charger-balance control and optimal-time control are similar same, at ~80 µs, the recovery time with optimal-time control is reduced by 25%. By comparison with the minimum charge-recovery time control, the improvement is therefore 75%. Similar results are observed for a load step down transient.

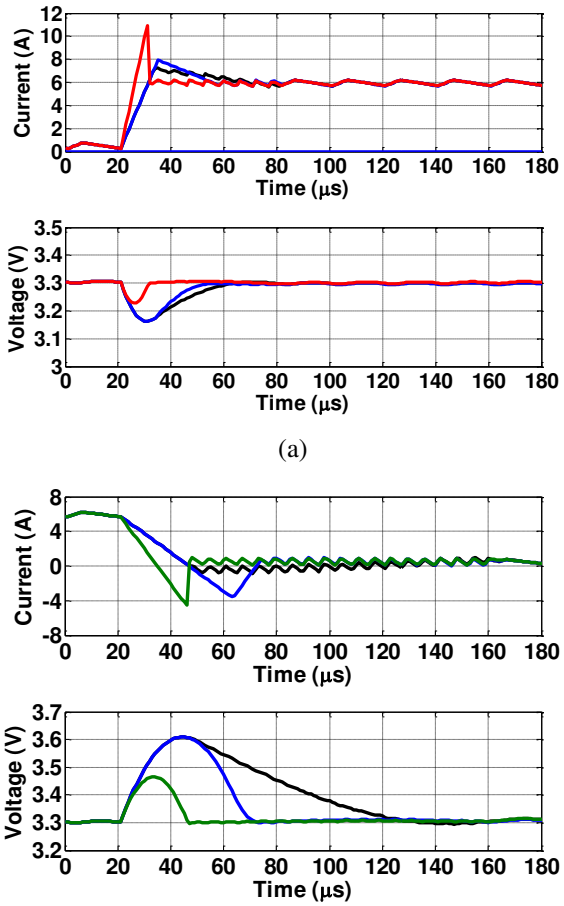

Fig. 9: Comparison of responses with charge-balance control to true optimal-time control. (a) current waveforms (b) output voltage

5 Conclusion

This paper has shown that optimal-time control can be achieved in a converter where the inductor ratio is smaller than the voltage ratio, extending this control scheme to a parallel connected converter which has one power module operating at a much higher switching frequency than the other power module. This paper also proposed the minimum charge-recovery time control which produces a recovery time that is faster than that in the optimal-time. The recovery time with the proposed scheme shows a reduction in charge recovery time by 75% in both load step -up and –down modes.

References

[1] R.P. Singh, A.M. Khambadkone. “A buck-derived topology with improved step-down transient performance”, IEEE Trans. Power Electron., **Vol. 23**, pp. 2855–2866, (2008).

[2] S. Lisheng, B.P. Baddipadiga, M. Ferdowsi, M.L. Crow. “Improving the dynamic response of a flying-capacitor three-level buck converter”, IEEE Trans. Power Electron., **Vol. 28**, pp. 2356-2365, (2013).

[3] L. Jia, Z. Hu, Y.-F. Liu, P.C. Sen, “Predictable auxiliary switching strategy to improve unloading transient response performance for DC-DC buck converter”, IEEE Trans. ind. Electron., **Vol. 49**, pp. 931-941, (2013).

[4] Y. Wen, and O. Trescases. “DC-DC converter with digital adaptive slope control in auxiliary phase for optimal transient response and improved efficiency”, IEEE APEC Conf., 2011, pp. 331-337, (2011).

[5] D.D.-C. Lu, J.C.P. Liu, F.N.K. Poon, B.M.H. Pong. “A single phase voltage regulator module (VRM) with stepping inductance for fast transient response”, IEEE Trans. Power Electron., **Vol. 22**, pp. 417-424, (2007).